JOC Article
pubs.acs.org/joc

Photochemistry of Fluorinated 4-Iodophenylnitrenes: Matrix Isolation and Spectroscopic Characterization of Phenylnitrene-4-yls

Dirk Grote and Wolfram Sander*

Lehrstuhl für Organische Chemie II der Ruhr-Universität, D-44780 Bochum, Germany

wolfram.sander@rub.de

Received May 29, 2009

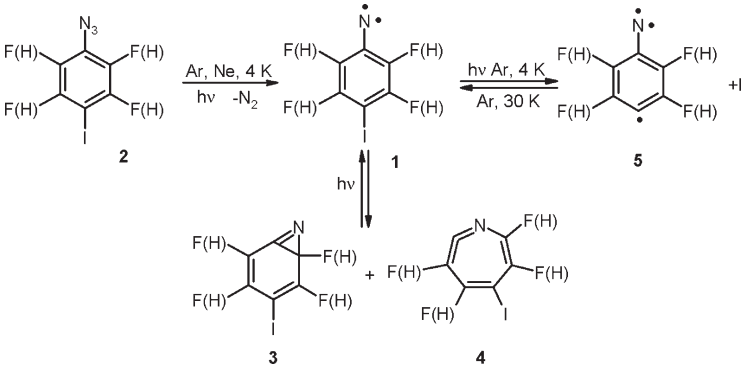

The photochemistry of a series of fluorinated *p*-iodophenyl azides **2** has been investigated using matrix isolation IR and EPR spectroscopy. In all cases, the corresponding phenylnitrenes **1** were formed as primary photoproducts. Further irradiation of the nitrenes **1** resulted in the formation of azirines **3**, ketenimines **4**, and nitreno radicals **5**. The yield of **5** depends on the number of *ortho* fluorine substituents: with two *ortho* fluorine atoms the highest yield is observed, whereas without fluorine atoms the yield is too low for IR spectroscopic detection. The interconversion between the isomers **1**, **3**, and **4** proved to be rather complex. If the fluorine atoms are distributed unsymmetrically, two isomers of azirines **3** and ketenimines **4** can be formed. The yields of these isomers depend critically on the irradiation conditions.

Introduction

Phenylnitrenes **1** are reactive intermediates with triplet ground states that have been extensively studied in recent years using matrix isolation spectroscopy and laser flash photolysis.[1] Phenylnitrenes **1** are conveniently generated by photolysis of the corresponding phenyl azides **2** which under loss of molecular nitrogen yield the singlet nitrenes **S-1** as the primary photoproducts. The fate of **S-1** with lifetimes in the order of several ns depends on the reaction conditions: they are either trapped by suitable reagents, deactivate to the ground state triplet nitrenes **T-1** via intersystem crossing, or rearrange to azirines **3** or ketenimines **4**.[2−4] During the last years, various arylnitrenes were investigated using matrix isolation spectroscopy, time-resolved UV−vis spectroscopy, and quantum chemical calculations.[5−11]

The mechanism of these nitrene rearrangements has been subject to controversial discussions for years, but due to extensive experimental and theoretical calculations the mechanism shown in Scheme 1 for the parent phenylnitrene **1a**

(1) Gritsan, N. P.; Platz, M. S. *Chem. Rev.* **2006**, *106*, 3844–3867.
(2) Hayes, J. C.; Sheridan, R. S. *J. Am. Chem. Soc.* **1990**, *112*, 5879–5881.
(3) Borden, W. T.; Gritsan, N. P.; Hadad, C. M.; Karney, W. L.; Kemnitz, C. R.; Platz, M. S. *Acc. Chem. Res.* **2000**, *33*, 765–771.
(4) Platz, M. S. In *Reactive Intermediate Chemistry*; Moss, R. A., Platz, M. S., Jones, M., Jr., Eds.; Wiley: New York, 2004.
(5) Maltsev, A.; Bally, T.; Tsao, M.-L.; Platz, M. S.; Kuhn, A.; Vosswinkel, M.; Wentrup, C. *J. Am. Chem. Soc.* **2004**, *126*, 237–249.
(6) Kvaskoff, D.; Bednarek, P.; George, L.; Pankajakshan, S.; Wentrup, C. *J. Org. Chem.* **2005**, *70*, 7947–7955.
(7) Vosswinkel, M.; Luerssen, H.; Kvaskoff, D.; Wentrup, C. *J. Org. Chem.* **2009**, *74*, 1171–1178.
(8) Kvaskoff, D.; Mitschke, U.; Addicott, C.; Finnerty, J.; Bednarek, P.; Wentrup, C. *Aust. J. Chem.* **2009**, *62*, 275–286.
(9) Kvaskoff, D.; Bednarek, P.; George, L.; Waich, K.; Wentrup, C. *J. Org. Chem.* **2006**, *71*, 4049–4058.
(10) Addicott, C.; Wong, M. W.; Wentrup, C. *J. Org. Chem.* **2002**, *67*, 8538–8546.
(11) Kuhn, A.; Vosswinkel, M.; Wentrup, C. *J. Org. Chem.* **2002**, *67*, 9023–9030.

Published on Web 09/04/2009 DOI: 10.1021/jo901145h

SCHEME 1. Rearrangement of Phenylnitrene 1a

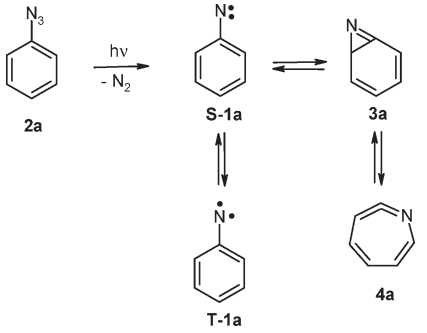

is now generally accepted. Irradiation of phenyl azide **2a**, matrix-isolated in argon at cryogenic temperatures, results in the formation of **1a**, **3a**, and **4a** in photostationary equilibria. According to ab initio calculations, singlet nitrene **S-1a** first rearranges to azirine **3a** via addition of the nitrogen atom to one of the neighboring aromatic C−C bonds. This rearrangement is slightly endothermic by 4 kcal/mol. Azirine **3a** subsequently opens up to the cyclic ketenimine **4a** which is 1.6 kcal/mol more stable than **S-1a**.[12] However, with a singlet−triplet splitting $\Delta E_{ST} = 18$ kcal/mol the triplet phenylnitrene **T-1a** is the most stable of these isomers.

Substituents in the *ortho* position, especially by fluorine atoms as in **1b** and **1c**, lead to a substantial increase in the activation barrier for the rearrangement to azirines **3** and thus to higher yields of singlet nitrene trapping products in solution.[1] The photochemistry of matrix-isolated 2,6-difluorophenylnitrene **T-1b** was investigated by several authors[13−15] but only recently could it be shown that indeed both **3b** and **4b** are formed in the photochemical rearrangement. The question why *ortho* fluorine substitution raises the barrier toward ring expansion of phenylnitrene has also been subject to a theoretical study.[16] Thus, phenyl azides bearing fluorine substituents in the *ortho* positions are the most suitable precursors for the generation of kinetically stabilized phenylnitrenes.

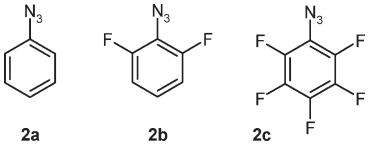

Introduction of an additional radical center in the phenyl ring leads to the interesting phenylnitrene-yls **5**−**7**. These nitreno radicals are characterized best as σ, σ, π triradicals with two unpaired σ electrons located at the nitrogen atom and the radical center of the phenyl ring, respectively, and the third unpaired electron being delocalized in the π system. The interaction between these three unpaired electrons

CHART 1. Phenyl Azides 2 Investigated in This Study

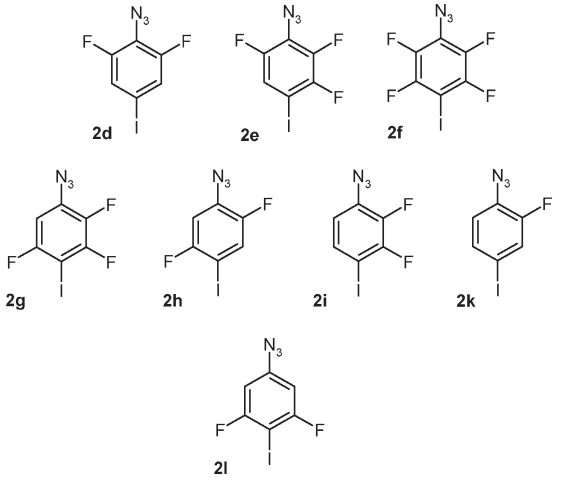

results in a number of close lying "low spin" (doublet) states and a "high spin" (quartet) state.

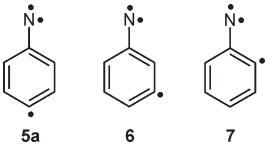

According to high-level ab initio calculations, in phenylnitrene-4-yl **5a** the quartet state is energetically preferred by 5.3 kcal/mol.[17] These calculations also predict a quartet ground state for phenylnitrene-2-yl **7**, whereas phenylnitrene-3-yl **6** is predicted to exhibit a low-spin doublet state as ground state.[18]

The only derivative of **5** that could be isolated and spectroscopically characterized, so far, is the perfluorinated triradical **5f** (Chart 1).[19] The IR spectrum of matrix-isolated **5f** is in good agreement with the spectrum calculated for the quartet state **Q-5f** but not with the lowest lying doublet state **D-5f**. The assignment of a quartet state for **5f** was later confirmed by EPR spectroscopy.[20] Here, we describe the matrix isolation and spectroscopic characterization (IR and EPR) of a series of new nitreno radicals **5**.

Results

The photochemistry of the eight *p*-iodophenyl azides **2d**−**l** has been investigated using matrix isolation spectroscopy with IR and EPR detection (Chart 1). In all cases, the primary photoproducts isolated in high yields were the corresponding triplet nitrenes **T-1**. The IR spectra of the nitrenes are in good agreement with DFT calculations at the UB3LYP/6-311G(d,p) level of theory. The EPR spectra show strong triplet signals with zfs parameters D and E as expected for phenylnitrenes (Table 1).

(12) Karney, W. L.; Borden, W. T. *J. Am. Chem. Soc.* **1997**, *119*, 1378–1387.
(13) Morawietz, J.; Sander, W. *J. Org. Chem.* **1996**, *61*, 4351–4354.
(14) Carra, C.; Nussbaum, R.; Bally, T. *ChemPhysChem* **2006**, *7*, 1268–1275.
(15) Mandel, S.; Liu, J.; Hadad Christopher, M.; Platz Matthew, S. *J. Phys. Chem. A* **2005**, *109*, 2816–21.
(16) Karney, W. L.; Borden, W. T. *J. Am. Chem. Soc.* **1997**, *119*, 3347–3350.
(17) Bettinger, H. F.; Sander, W. *J. Am. Chem. Soc.* **2003**, *125*, 9726–9733.
(18) Sander, W.; Winkler, M.; Cakir, B.; Grote, D.; Bettinger, H. F. *J. Org. Chem.* **2007**, *72*, 715–724.
(19) Wenk, H. H.; Sander, W. *Angew. Chem., Int. Ed.* **2002**, *41*, 2742–2745.
(20) Sander, W.; Grote, D.; Kossmann, S.; Neese, F. *J. Am. Chem. Soc.* **2008**, *130*, 4396–4403.

TABLE 1. zfs Parameters of the Triplet and Quartet Species (g_{iso} = 2.003)

	T-1			Q-5	
fluorine distribution	$\|D/hc\|$ (cm^{-1})	$\|E/hc\|$ (cm^{-1})	nitrogen spin density[a]	$\|D/hc\|$ (cm^{-1})	$\|E/hc\|$ (cm^{-1})
2,3,6- (**e**)	0.981	0.0071	1.5725	0.289	0.041
2,6- (**d**)	0.925	0.0086	1.5694	0.291	0.040
2,3,5,6- (**f**)	1.103	0.0120	1.5762	0.285	0.043
2,3,5- (**g**)	1.073	0.0091	1.5792	0.283	0.042
2,5- (**h**)	0.954	0.0120	1.5689	0.278	0.040
2,3- (**i**)	0.953	0.0032	1.5782	0.287	0.040
2- (**k**)	0.900	0.0036	1.5712	0.285	0.040
3,5- (**l**)	1.053	0.0103	1.5852		

[a]UB3LYP/6-311G(d,p).

SCHEME 2. Photochemistry of 2d

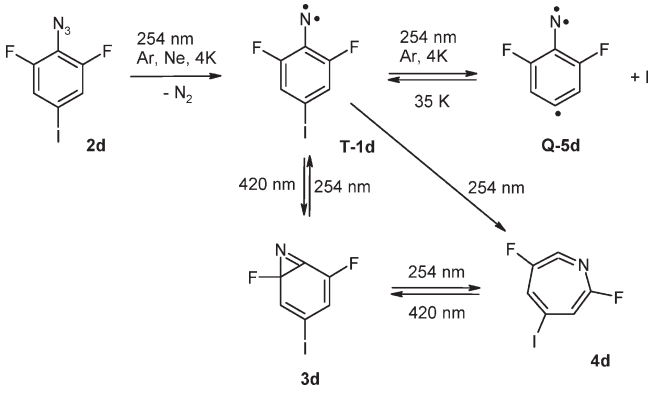

SCHEME 3. Photochemistry of 2e

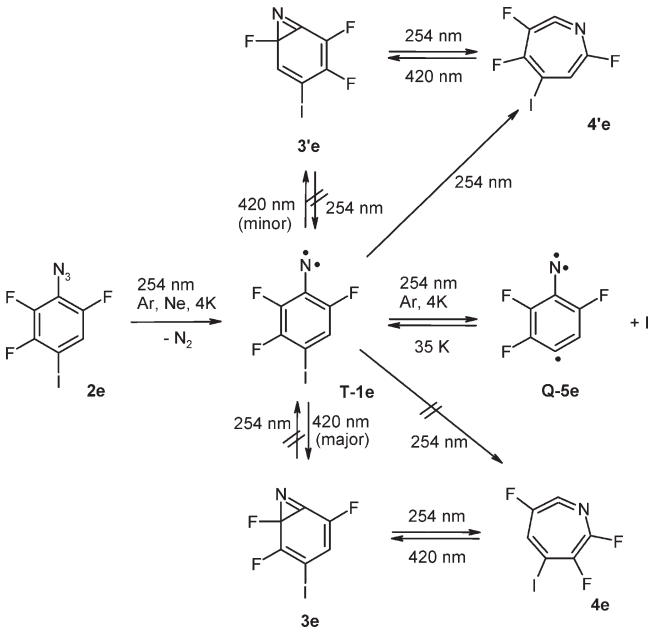

Irradiation of the nitrenes **T-1** produced complex product mixtures with a composition much depending on the light source (UV or visible light, narrow or broadband irradiation), the matrix temperature (between 3 and 15 K), and the matrix host (neon or argon). Three basic types of substitution patterns in the precursor molecules will be discussed separately: (i) phenyl azides bearing two fluorine atoms in the *ortho* positions **2d**−**f**, (ii) one fluorine and one hydrogen atom **2g**−**k**, and (iii) two hydrogen atoms **2l**. For each of these classes of phenyl azides one representative will be presented in detail, while for the other precursors only deviations from the general scheme will be discussed.

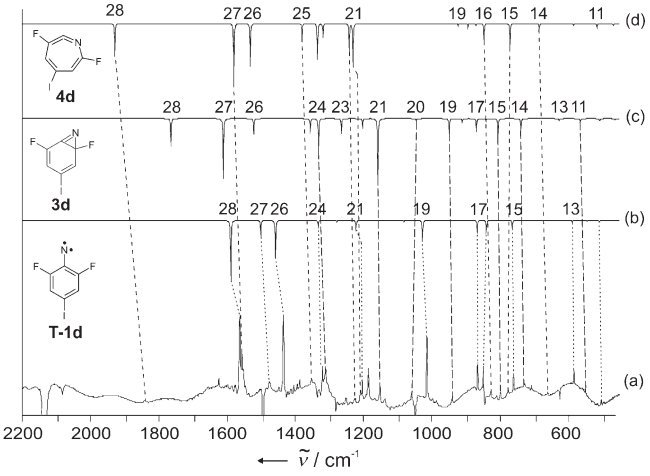

FIGURE 1. IR spectra showing the 320 nm photochemistry of azide **2d** in argon at 4 K. (a) Difference IR spectrum: bands pointing downward disappear during irradiation and are assigned to **2d**; bands pointing upward appear and are assigned to the photoproducts **T-1d** (major product), **3d**, and **4d**. (b) Calculated IR spectrum of **T-1d** (c) Calculated IR spectrum of **3d**. (d) Calculated IR spectrum of **4d**. All calculations at the (U)B3LYP/6-311G(d,p) level of theory.

Photochemistry of 2,6-Difluoro-4-iodophenyl Azide 2d. The photochemistry of **2d**, **2e**, and **2f** (which was described previously)[19,20] with two fluorine atoms in the *ortho* positions is very similar, and here we focus on **2d** as a representative sample (Scheme 2). The photochemistry of **2e** is complicated by the asymmetric distribution of the fluorine substituents which increases the number of the isomers formed during photolysis (Scheme 3).

UV irradiation ($\lambda = 254$ or > 320 nm) of phenyl azide **2d** in solid argon or neon at 4 K results in a rapid decrease of all IR absorptions of the azide and formation of a new main product with very strong IR bands at 1562.9, 1476.2, 1434.2, and 1013.4 cm^{-1} assigned to nitrene **T-1d**. DFT calculations (UB3LYP/6-311G(d,p)) predict the strongest IR absorptions of **T-1d** at 1589.6, 1502.0, 1458.1, and 1027.4 cm^{-1} (unscaled), in very good agreement with the experiment (Figure 1). The EPR spectrum of **T-1d** is characteristic of a triplet phenylnitrene with zero field splitting (zfs) parameters $|D/hc| = 0.925$ cm^{-1} and $|E/hc| = 0.0086$ cm^{-1}.[20]

A second product that is formed during the UV irradiation is didehydroazepine (ketenimine) **4d** with a characteristic strong IR absorption at 1840.7 cm^{-1}, assigned to the N=C=C str. vibration (Table 2). Absorptions in this range

TABLE 2. IR Spectroscopic Data of 4 and 4′, Matrix-Isolated in Argon at 4 K

	ν(C=C=N) 4'			ν(C=C=N) 4	
	$\tilde{\nu}_{exp.}$/cm^{-1} ($I_{rel.,\,exp}$)[a]	$\tilde{\nu}_{calc.}$/cm^{-1} ($I_{rel.,\,calc}$)[b]		$\tilde{\nu}_{exp.}$/cm^{-1} ($I_{rel.,\,exp}$)[a]	$\tilde{\nu}_{calc.}$/cm^{-1} ($I_{rel.,\,calc}$)[b]
f	-	-		1854.1[d] (0.16)	1930.3 (0.33)
e	 1857.4 (0.52)	1937.0 (0.45)		-	1920.3 (0.54)
d	-	-		1840.7 (1.00)	1929.1 (0.56)
g	 1869.4[d] (0.05)	1940.1 (0.60)		1878.5 (1.00)	1950.3 (1.00)
h	-	-		1888.3 (0.87)	1959.2 (0.87)
i	 1873.7 (-)[c]	1948.5 (0.40)		1873.7 (-)[c]	1949.9 (1.00)
k	 -	-		1878.1 (0.06) 1888.1 (0.18)	1958.9 (1.00)
l	 1892.5 (1.00)	1961.7 (1.00)		-	-

[a]Argon, 4 K. [b]B3LYP/6-311G(d,p), unscaled. Relative intensities based on the strongest absorption. [c]Overlap with other bands. [d]Neon, 4 K.

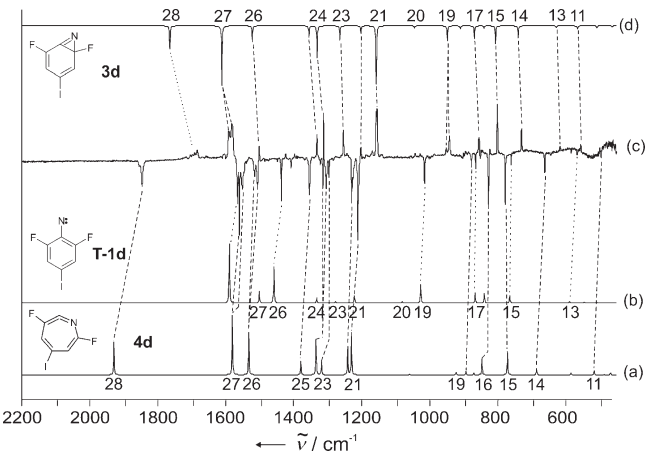

FIGURE 2. IR spectra showing the photochemical interconversion between **T1-d**, **3d**, and **4d** during 420 nm irradiation in argon at 4 K. (a) Calculated IR spectrum of **4d**. (b) Calculated IR spectrum of **T-1d**. (c) Difference IR spectrum: bands pointing upward are appearing and assigned to **3d**; bands pointing downward disappear and are assigned to **T1-d** and **4d**. (d) Calculated IR spectrum of **3d**. All calculations at the (U)B3LYP/6-311G(d,p) level of theory.

have been reported for a number of didehydroazepines; e.g., **4a** shows a strong band at 1895 cm^{-1} and **4b** at 1830 cm^{-1}.[14] DFT calculations predict the N=C=C str vibration of **4d** at 1929.1 cm^{-1}, which is considerably blue-shifted compared to the experimental value, while the other vibrations of **4d** are in good agreement with the experiment. The large error for the

TABLE 3. IR Spectroscopic Data of Azirines 3 and 3′, Matrix-Isolated in Argon at 4 K

	ν(C=N) 3'			ν(C=N) 3	
	$\tilde{\nu}_{exp.}$/cm^{-1} ($I_{rel.,\,exp}$)[a]	$\tilde{\nu}_{calc.}$/cm^{-1} ($I_{rel.,\,calc}$)[b]		$\tilde{\nu}_{exp.}$/cm^{-1} ($I_{rel.,\,exp}$)[a]	$\tilde{\nu}_{calc.}$/cm^{-1} ($I_{rel.,\,calc}$)[b]
f	-	-		-	-
e	 1703.5 (0.02)	1765.2 (0.34)		1685.1 (0.06)	1766.4 (0.22)
d	-	-		1680.8 (0.06)	1765.0 (0.39)
g	 1720.0 (0.12)	1801.3 (0.41)		1711.5 (0.09)	1784.2 (0.16)
h	 1718.1 (0.08)	1800.9 (0.36)		1694.0 (0.33)	1781.1 (0.17)
i	 1709.3 (0.03)	1800.6 (0.45)		1692.9 (0.01)	1779.9 (0.18)
k	 1722.3 (0.11)	1802.1 (0.30)		-	1779.9 (0.53)
l	 1739.1 (0.08)	1821.6 (0.53)		-	-

[a]Argon, 4 K; [b]B3LYP/6-311G(d,p), unscaled. Relative intensity based on the strongest absorption.

calculation of the N=C=C str vibration is also observed in other ketenimines.

Azirine **3d** is also found in the product mixture after irradiation of **2d** upon $\lambda > 320$ nm. The azirine was identified by comparison of its IR spectrum with that of **3b** and other related azirines and with results from DFT calculations. A characteristic absorption of **3d** is the C=N stretching vibration at 1680.8 cm^{-1} (Table 3). Irradiation of a product mixture formed on irradiation of precursor **2d** with visible light ($\lambda >$ 420 nm) results in a decrease of **4d** and **T-1d** and an increase of **3d** (Figure 2). A careful analysis of the relative amounts of **1d**, **3d**, and **4d** reveals that on broadband UV irradiation ($\lambda > 320$ nm) these products are formed in photostationary equilibria with **1d** and **4d** being the major products. However, the photochemistry is much more selective with 254 nm; here only **1d** and **4d** but no **3d** are formed (Scheme 2).

Prolonged 254 nm irradiation (argon, 4 K) of the product mixture produces a further compound with IR bands at 1405.5, 1326.2, 1185.3, 997.9, and 814.3 cm^{-1} (Table 4) which is in better agreement with calculations for quartet triradical **Q-5d** than for doublet **D-5d**. However, the differences between the calculated spectra of **Q-5d** and **D-5d** are not very pronounced (Figure 3), and the assignment is therefore based on the EPR spectra. This is different to the tetrafluorinated system **5f** where the differences in the IR spectra calculated for the quartet state and the doublet state are large enough for an assignment based on the IR spectra.[19]

TABLE 4. IR Spectroscopic Data of 5d, Matrix-Isolated in Argon at 4 K, Compared to Calculations for the Quartet and Doublet State

	Ar, 4 K		Q-5d		D-5d
mode	$\tilde{\nu}_{exp}/cm^{-1}$ $(I_{rel,exp})^b$	symmetry	$\tilde{\nu}_{calcd}/cm^{-1}$ ^{a} $(I_{rel,calcd})^{a,b}$	symmetry	$\tilde{\nu}_{calcd}/cm^{-1a}$ $(I_{rel,calcd})^{a,b}$
13	814.3 (0.14)	b_1	814.8 (0.30)	b_1	811.0 (0.26)
14		a_1	820.3 (0.02)	a_1	820.9 (0.02)
15		a_2	835.1 (0.00)	a_2	847.7 (0.00)
16	997.9 (0.84)	b_2	1010.1 (0.51)	b_2	1014.0 (0.43)
17		a_1	1048.7 (0.03)	a_1	1059.3 (0.02)
18	1185.3 (0.35)	b_2	1186.9 (0.18)	b_2	1185.2 (0.18)
19		a_1	1253.7 (0.03)	a_1	1246.8 (0.00)
20		b_2	1287.6 (0.04)	b_2	1267.9 (0.00)
21	1326.2 (0.32)	a_1	1327.3 (0.17)	a_1	1305.0 (0.19)
22		a_1	1360.0 (0.00)	a_1	1371.4 (0.00)
23	1405.5 (1.00)	b_2	1426.9 (1.00)	b_2	1415.8 (1.00)
24		b_2	1534.9 (0.20)	a_1	1553.6 (0.56)
25		a_1	1541.1 (0.66)	b_2	1554.7 (0.22)

^{a}UB3LYP/6-311G(d,p), unscaled. ^{b}Relative intensity based on the strongest absorption.

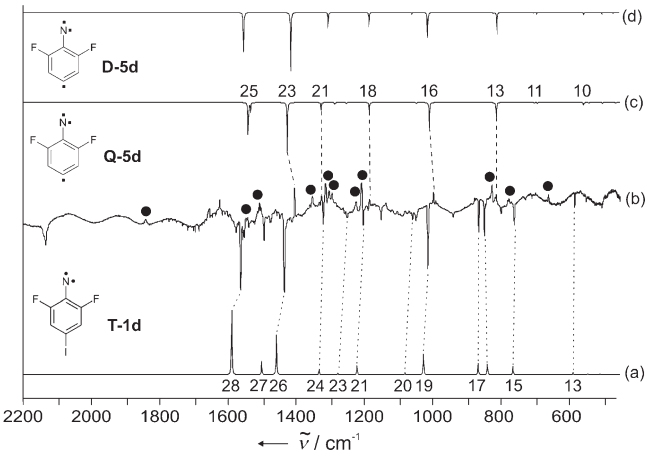

FIGURE 3. IR spectra showing the 254 nm photochemistry of nitrene **T-1d** in argon at 4 K. (a) Calculated IR spectrum of **T-1d**. (b) Difference spectrum: bands pointing downward disappear; bands pointing upward appear during irradiation. Bands marked with ● assigned to **4d**. (c) Calculated IR spectrum of quartet **Q-5d**. (d) Calculated IR spectrum of doublet **D-5d**. All calculations at the (U)B3LYP/6-311G(d,p) level of theory.

The EPR spectrum of matrix-isolated **5d** obtained after UV irradiation of **2d** allows a definitive assignment of the quartet spin state **Q-5d**. The spectrum shows a pattern characteristic of a quartet spin state with zfs parameters $|D/hc| = 0.291\ cm^{-1}$ and $|E/hc| = 0.040\ cm^{-1}$ (Figure 4). The EPR spectrum of **Q-5d** is very similar to that obtained for **Q-5f** which was discussed in detail elsewhere.[20]

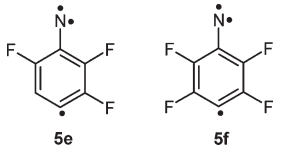

Irradiation with visible light reduces the amount of **5d** in the matrix. Presumably, this irradiation leads to local heating of the matrix and thermal recombination of **5d** with iodine atoms in proximity. The matrix and temperature effects controlling the formation of **5d** are very subtle and not yet understood. Thus, photolysis of **1d** in argon at 10 K or in neon at 4 K produces only very low yields of **5d**. The highest yields are observed in solid argon at 4 K.

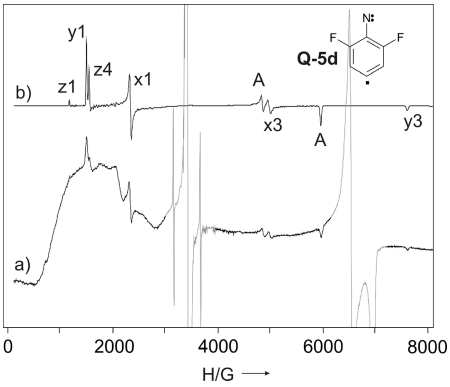

FIGURE 4. (a) EPR spectrum of **Q-5d** (argon, 4 K) formed after 308 nm irradiation of **2d**. (b) Simulated spectrum using $S = 3/2$, $|D/hc| = 0.291\ cm^{-1}$, and $|E/hc| = 0.040\ cm^{-1}$. The intense signal between 6500 and 7000 G is assigned to **T-1d**.

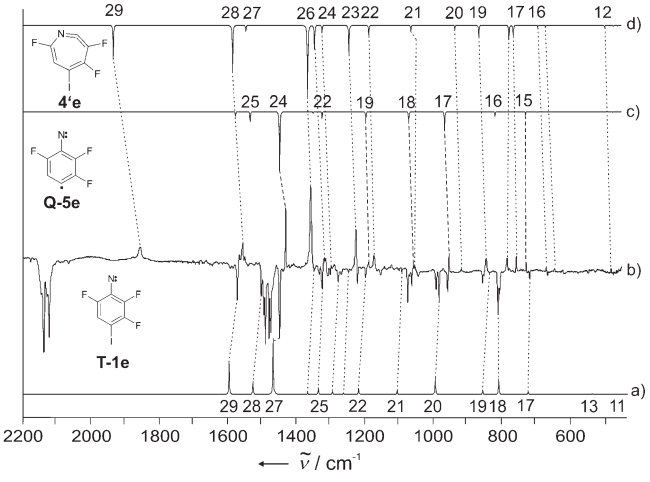

FIGURE 5. IR spectra showing the 254 nm photochemistry of nitrene **T-1e** in argon at 4 K after 47 min of irradiation. (a) Calculated IR spectrum of nitrene **T-1e**. (b) Difference IR spectrum: bands of **T-1e** pointing downward disappear; bands pointing upward assigned to **Q-5e** and **4′e** appear during irradiation. (c) Calculated IR spectrum of **Q-5e**. (d) Calculated IR spectrum of **4′e**. The second isomer **4e** is not observed. All calculations at the (U)B3LYP/6-311G(d,p) level of theory.

Due to the asymmetric fluorine substitution, the rearrangement of nitrene **1e** can principally produce the two isomeric azirines **3e** and **3′e** and the two isomeric ketenimines **4e** and **4′e**. Irradiation of **T-1e** with UV light (254 nm) produces **4′e** as the major product, but almost no **4e** (Figure 5). In contrast, visible light irradiation ($\lambda >$ 420 nm) of **T-1e** yields **3e** as the major product and only traces of **3′e**. However, if a matrix containing ketenimine **4′e** is irradiated with visible light, azirine **3′e** is produced as a major product. On the other hand, UV irradiation of a matrix containing azirine **3e** produces ketenimine **4e** as a major product (Figure 6). Thus, depending on the sequence of UV and visible light irradiation, the isomeric azirine **3e** or the isomeric ketenimine **4′e** is obtained as major product. This puzzling photochemical behavior will be discussed later.

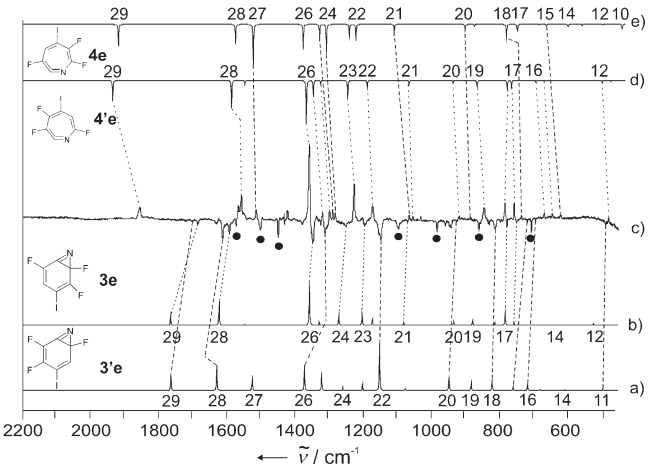

FIGURE 6. IR spectra showing the 254 nm photochemistry of nitrene **T-1e** in argon at 4 K after 10 min of irradiation. (a) Calculated IR spectrum of **3′e**. (b) Calculated IR spectrum of **3e**. (c) Difference IR spectrum: bands of **3e** and **3′e** pointing downward disappear, bands pointing upward assigned to **4e** and **4′e** appear during irradiation. Bands marked with ● assigned to **T-1e**. (d) Calculated IR spectrum of **4′e**. (e) Calculated IR spectrum of **4e**. All calculations at the (U)B3LYP/6-311G(d,p) level of theory.

TABLE 5. IR Spectroscopic Data of 5e, Matrix-Isolated in Argon at 4 K, Compared to Calculations for the Quartet and the Doublet State

	Ar, 4 K		Q-5e		D-5e
mode	$\tilde{\nu}_{calcd}$/cm^{-1} ($I_{rel,exp}$)^b	symmetry	$\tilde{\nu}_{exp}$/cm^{-1a} ($I_{rel,calcd}$)^{a,b}	symmetry^c	$\tilde{\nu}_{calcd}$/cm$^{-1\ a}$ ($I_{rel,calcd}$)^{a,b}
14		a'	695.6 (0.01)		696.1 (0.01)
15	727.3 (0.22)	a'	729.5 (0.06)		728.3 (0.05)
16		a'	818.5 (0.08)		823.8 (0.07)
17	953.0 (0.83)	a'	966.8 (0.27)		968.5 (0.23)
18	1057.3 (0.25)	a'	1071.6 (0.14)		1075.0 (0.12)
19	1188.7 (0.11)	a'	1197.1 (0.14)		1192.9 (0.10)
20		a'	1263.6 (0.00)		1262.0 (0.03)
21		a'	1294.9 (0.00)		1270.2 (0.04)
22		a'	1325.9 (0.12)		1308.3 (0.09)
23		a'	1351.7 (0.03)		1359.2 (0.02)
24	1431.0 (1.00)	a'	1449.1 (1.00)		1442.1 (1.00)
25		a'	1541.1 (0.66)		1550.9 (0.15)
26		a'	1578.5 (0.09)		1595.1 (0.05)

[a]UB3LYP/6-311G(d,p), unscaled. [b]Relative intensity based on the strongest absorption. [c]Calculation performed with C_1 symmetry.

The quartet nitreno radical **Q-5e** with a characteristic IR absorption at 1431 cm^{-1} is formed as a minor product during prolonged 254 nm irradiation (Table 5). **Q-5e** is also formed in a neon matrix, but the yield is much lower than in solid argon. Annealing of an argon matrix containing **Q-5e** at 30 K or irradiation with $\lambda > 420$ nm results in recombination of the iodine atom with **5e** producing nitrene **1e** or azirine **3e**.

Photochemistry of 2,5-Difluoro-4-iodophenyl Azide 2h. The photochemistry of the azides **2g**, **2h**, **2i**, and **2k** bearing only one *ortho* fluorine substituent is very similar. The asymmetric fluorine substitution leads to two isomeric azirines **3** and **3′** and ketenimines **4** and **4′** which are formed in variable amounts depending on the experimental conditions. The overall trend in the selectivity of the formation of these products is quite similar in all four systems; we therefore focus on the photochemistry of **2h** as a prototype (Scheme 4).

UV irradiation (λ = 254 nm) of phenyl azide **2h** in solid argon or neon at 4 K results in a rapid decrease of all IR

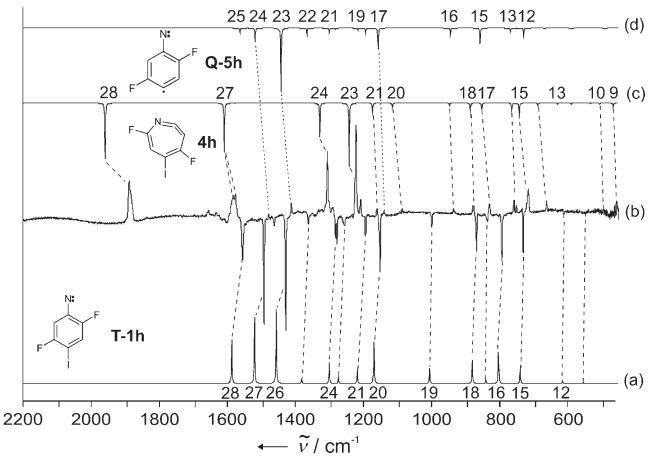

FIGURE 7. IR spectra showing the 254 nm photochemistry of nitrene **T-1h** in argon at 4 K after 80 min of irradiation. (a) Calculated IR spectrum of **T-1h**. (b) Difference IR spectrum: bands of **T-1h** pointing downward disappear; bands pointing upward assigned to **Q-5h** and **4h** appear during irradiation. The second ketenimine **4′h** is not observed. (c) Calculated IR spectrum of **4h**. (d) Calculated IR spectrum of **Q-5h**. All calculations at the (U)B3LYP/6-311G(d,p) level of theory.

SCHEME 4. Photochemistry of 2h

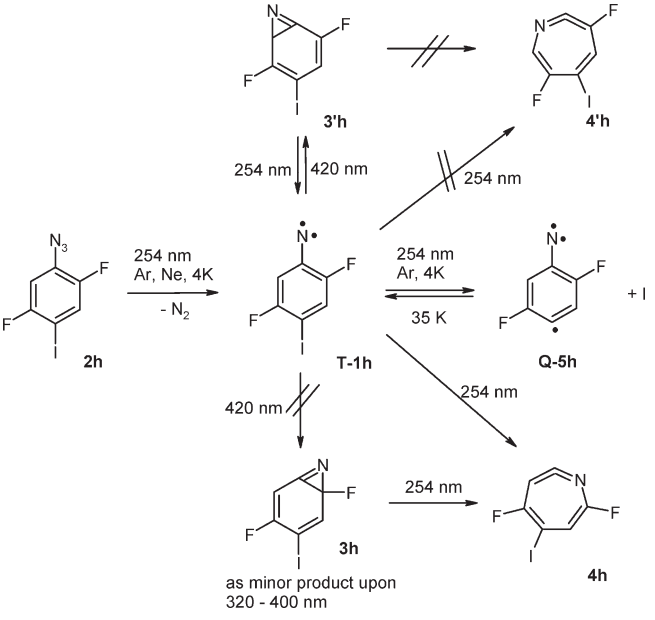

absorptions of the azide and formation of a new product with three characteristic bands at 1555.0, 1492.2, and 1428.6 cm^{-1} (in argon). The new product was assigned to triplet nitrene **T-1h** by comparison of the IR spectrum with DFT calculations at the UB3LYP/6-311G(d,p) level of theory. The EPR spectrum of **T-1h** with $|D/hc| = 0.954$ cm^{-1} and $|E/hc| = 0.012$ cm^{-1} is characteristic of triplet phenylnitrenes and in line with the other nitrenes investigated in this study (Table 1).

Short irradiation times of the precursor leads to **T-1h** exclusively. However, during prolonged UV irradiation two new sets of IR bands are formed while all bands assigned to **T-1h** decrease. A characteristic band at 1888.3 cm^{-1} (argon, 4 K) is assigned to the N=C=C str vibration of a ketenimine **4**. A closer investigation reveals that only isomer

TABLE 6. IR Spectroscopic Data of 5h, Matrix-Isolated in Argon at 4 K, Compared to Calculations for the Quartet and the Doublet State

	Ar, 4 K		Q-5h		D-5h
mode	$\tilde{\nu}_{exp}/cm^{-1}$ ($I_{rel,exp}$)[b]	symmetry	$\tilde{\nu}_{calcd}/cm^{-1}$[a] ($I_{rel,calcd}$)[a,b]	symmetry	$\tilde{\nu}_{calcd}/cm^{-1}$[a] ($I_{rel,\ calcd}$)[a,b]
12		a′	729.4 (0.12)	a′	728.6 (0.11)
13		a′	768.7 (0.06)	a′	774.6 (0.05)
14		a″	818.0 (0.00)	a″	821.7 (0.00)
15		a′	857.9 (0.25)	a″	857.7 (0.20)
16		a′	944.8 (0.11)	a′	949.4 (0.11)
17	1139.3 (0.39)	a′	1157.8 (0.34)	a′	1160.2 (0.33)
18		a′	1194.2 (0.08)	a′	1196.6 (0.04)
19		a′	1216.3 (0.04)	a′	1212.6 (0.01)
20		a′	1282.5 (0.01)	a′	1262.5 (0.05)
21		a’	1300.3 (0.08)	a′	1280.2 (0.02)
22		a′	1366.3 (0.10)	a′	1357.9 (0.13)
23	1411.4 (1.00)	a′	1443.0 (1.00)	a′	1436.5 (1.00)
24	1478.5 (0.61)	a′	1518.2 (0.22)	a′	1532.8 (0.13)
25		a′	1563.6 (0.08)	a′	1581.5 (0.06)

[a]UB3LYP/6-311G(d,p), unscaled. [b]Relative intensity based on the strongest absorption.

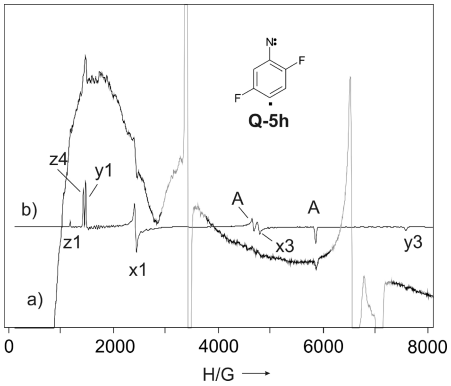

FIGURE 8. (a) EPR spectrum of **Q-5h** (argon, 15 K) formed after 308 nm irradiation of **T-1h**. (b) Spectrum simulated with $S = 3/2$, $|D/hc| = 0.278\ cm^{-1}$, $|E/hc| = 0.040\ cm^{-1}$, and $g = 2.003$. Due to slightly smaller zfs parameters, z4 appears as shoulder on the low field side of y1.

4h is formed, while **4′h** is not observed (Figure 7). Thus, the nitrogen atom of nitrene **T-1h** is inserting into the C−C bond bearing the fluorine substituent.

The most intense band of the remaining IR absorptions at 1411.4 cm^{-1} is assigned to nitreno radical **5h**. For the quartet and the doublet state of **5h**, DFT calculations (UB3LYP/6-311G(d,p)) predict bands at 1443.0 and 1436.5 cm^{-1}, respectively, which are too close to allow an assignment (Table 6). However, the EPR spectrum clearly shows a quartet system **Q-5h** with zfs parameters $|D/hc| = 0.278\ cm^{-1}$ and $|E/hc| = 0.040\ cm^{-1}$, similar to that of **Q-5f** (Figure 8).

Upon irradiation with visible light ($\lambda > 420$ nm), the IR absorptions of **1h** and **5h** decrease while new bands appear in the spectrum. These new absorptions were identified as **3′h** by comparison with DFT calculations (Supporting Information, Figure S4). The most characteristic absorption is the C=N stretching vibration at 1718.1 cm^{-1} (argon, 4 K). The decrease of nitreno radical **5h** upon visible light irradiation is most likely caused by local heating of the matrix resulting in a thermal recombination of **5h** with an iodine atom. Azirine **3h** is obtained in small amounts during 320−400 nm irradiation (Figure 9).

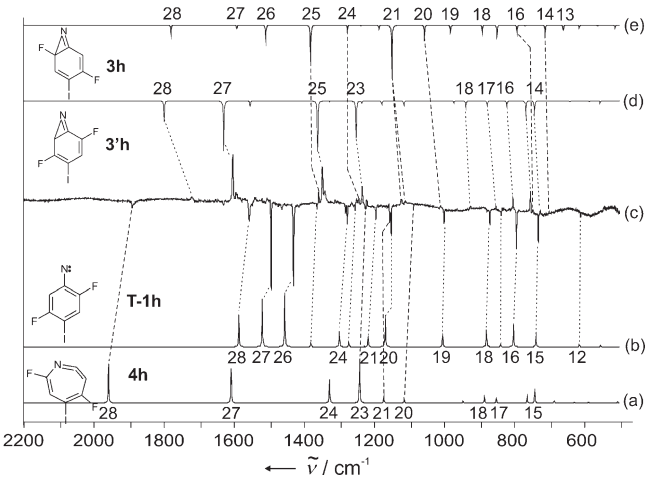

FIGURE 9. IR spectra showing the 320−400 nm photochemistry of nitrene **T-1h** and ketenimine **4h** in argon at 4 K after 10 min of irradiation. (a) Calculated IR spectrum of **4h**. (b) Calculated IR spectrum of **T-1h**. (c) Difference IR spectrum: bands of **T-1h** pointing downward disappear; bands pointing upward assigned to **3h** and **3′h** appear during irradiation. (d) Calculated IR spectrum of **3′h**. (e) Calculated IR spectrum of **3h**. All calculations at the (U)B3LYP/6-311G(d,p) level of theory.

UV photolysis of azides **2g**, **2i**, and **2k** results in the expected formation of the corresponding triplet nitrenes **T-1** as primary products in high yields. However, while the further photochemistry of **1g** and **1k** shows a quite similar selectivity than that of **1h**, the photochemistry of **1i** upon UV irradiation is much less selective. UV irradiation ($\lambda = 254$ nm) of the nitrenes **1g** and **1k** results in the selective rearrangement to ketenimines **4g** and **4k**, respectively. Thus, as with **1h**, the nitrogen atoms insert selectively into the adjacent C−C bonds bearing the fluorine substituents. Only traces of the isomer **4′g**, but not of **4′k**, are found. In contrast, UV photolysis of **1i** shows no selectivity, and both **4i** and **4′i** are formed in similar yields. The photochemistry of **2g** is summarized in Scheme 5.

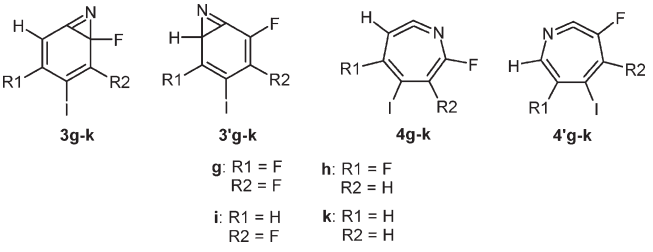

Subsequent irradiation of the product mixtures obtained by UV irradiation of **1g**, **1k**, and **1i** with visible light ($\lambda >$ 420 nm) results in the formation of **3′g**, **3′k**, and **3′i**, respectively, as the major products. These products are formed by a formal addition of the nitrene nitrogen atom to the adjacent C−C bond without fluorine substitution. The selectivity of this rearrangement is high; only small amounts of **3i** but no **3k** are observed under these conditions. For **3g**, this selectivity is still apparent, but less striking (Supporting Information, Figure S1). While the irradiation of nitrenes with visible light yields higher amounts of azirine **3′i** (Supporting Information, Figure S2), **3′h**, **3′k**, and **3′g**, the

SCHEME 5. Photochemistry of 2g

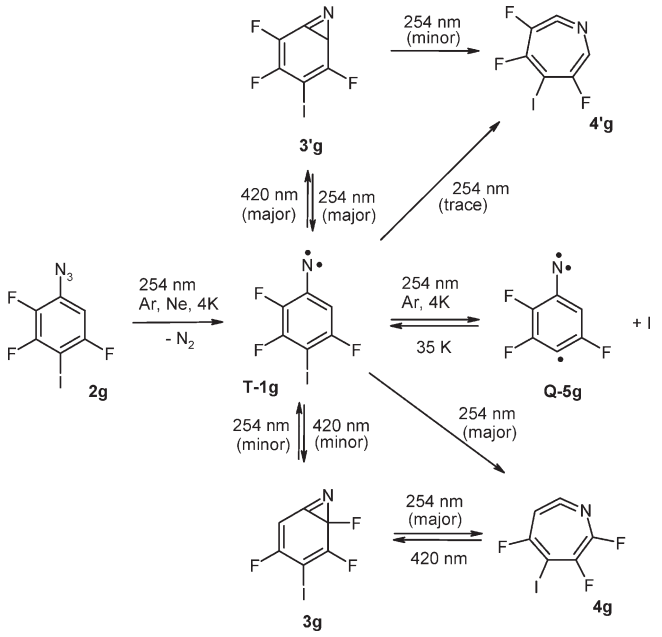

TABLE 7. IR Spectroscopic Data of 5g, Matrix-Isolated in Argon at 4 K, Compared to Calculations for the Quartet and the Doublet State

	Ar, 4 K		Q-5g		D-5g
mode	$\tilde{\nu}_{exp}/cm^{-1}$ $(I_{rel,exp})^b$	symmetry	$\tilde{\nu}_{calcd}/cm^{-1a}$ $(I_{rel,calc})^{a,b}$	symmetry	$\tilde{\nu}_{calcd}/cm^{-1a}$ $(I_{rel,\ calc})^{a,b}$
15		a′	772.2(0.11)	a′	774.9(0.14)
16		a″	822.2 (0.14)	a″	810.9 (0.13)
17	1002.3 (0.88)	a′	1014.6 (0.33)	a′	1015.7 (0.42)
18	1061.9 (0.38)	a′	1072.9 (0.48)	a′	1074.8 (0.54)
19		a′	1177.0 (0.08)	a′	1170.5 (0.14)
20		a′	1217.0 (0.03)	a′	1219.6 (0.02)
21		a′	1306.3 (0.00)	a′	1278.8 (0.09)
22		a′	1323.7 (0.32)	a′	1302.7 (0.40)
23		a′	1401.4 (0.11)	a′	1409.5 (0.65)
24	1408.5 (1.00)	a′	1428.1 (1.00)	a′	1428.5 (1.00)
25		a′	1555.2 (0.23)	a′	1563.1 (0.28)
26		a′	1564.7 (0.60)	a′	1584.9 (0.62)

[a]UB3LYP/6-311G(d,p), unscaled. [b]Relative intensity based on strongest absorption.

azirines **3g** and **3i** are obtained by visible light irradiation from the corresponding ketenimines **4g** and **4i**. This photochemical rearrangement is most selective for **4g** (Supporting Information, Figure S3). Compound **3k** is not formed at all.

In analogy to nitrene **1h**, prolonged UV irradiation of the nitrenes **1g**, **1i**, and **1k** produces the corresponding nitreno radicals **5** which were characterized by their IR and EPR spectra. In all three cases, the EPR spectra correspond to quartet systems **Q-5** (Tables 7−9). The EPR spectra could be simulated with the zfs parameters given in Table 1.

Photochemistry of 3,5-Difluoro-4-iodophenylazide 2l. UV irradiation ($\lambda = 254$ nm) of **2l** in solid argon or neon at 4 K results in the rapid decrease of the IR absorptions of the azide (Scheme 6). Simultaneously, new intense absorptions are formed at 1507.9 and 1300.6 cm^{-1} (argon, 4 K) which are assigned to **T-1l** by comparison with UB3LYP/6-311G(d,p) calculations (Figure 10). The EPR spectrum shows the formation of a triplet system with zfs parameters $|D/hc| = 1.053$ and $|E/hc| = 0.0103$ cm^{-1}.

TABLE 8. IR Spectroscopic Data of 5i, Matrix-Isolated in Argon at 4 K, Compared to Calculations for the Quartet State

	Ar, 4 K		Q-5i
mode	$\tilde{\nu}_{exp}/cm^{-1}$ $(I_{rel,exp})^b$	symmetry	$\tilde{\nu}_{calcd}/cm^{-1a}$ $(I_{rel,calc})^{a,b}$
12		a′	702.0 (0.20)
13		a″	766.9 (0.41)
14		a′	804.2 (0.05)
15		a″	934.0 (0.00)
16	1007.9 (0.50)	a′	1024.5 (0.62)
17		a′	1111.7 (0.23)
18	1159.7 (0.23)	a′	1175.3 (0.28)
19		a′	1225.6 (0.31)
20		a′	1299.6 (0.03)
21		a′	1316.2 (0.47)
22		a′	1405.5 (0.49)
23	1400.6 (0.31)	a′	1425.8 (1.00)
24		a′	1525.8 (0.35)
25	1536.0 (1.00)	a′	1563.0 (0.99)

[a]UB3LYP/6-311G(d,p), unscaled. [b]Relative intensity based on strongest absorption.

TABLE 9. IR Spectroscopic Data of 5k, Matrix-Isolated in Argon at 4 K, Compared to Calculations for the Quartet and the Doublet State

	Ar, 4 K		Q-5k		D-5k
mode	$\tilde{\nu}_{exp}/cm^{-1}$ $(I_{rel,exp})^b$	symmetry	$\tilde{\nu}_{calc}/cm^{-1a}$ $(I_{rel,calc})^{a,b}$	symmetry	$\tilde{\nu}_{calcd}/cm^{-1a}$ $(I_{rel,calcd})^{a,b}$
6	513.5 (0.46)	a′	520.2 (0.20)	a″	459.9 (0.01)
7		a″	552.1 (0.05)	a′	519.3 (0.14)
8		a′	567.1 (0.03)	a′	567.2 (0.02)
9		a″	688.7 (0.00)	a″	679.0 (0.02)
10	750.4 (0.15)	a′	763.5 (0.21)	a′	769.1 (0.18)
11	766.6 (0.23)	a″	782.0 (0.74)	a″	779.0 (0.73)
12		a′	838.1 (0.11)	a′	838.3 (0.09)
13		a″	839.6 (0.47)	a″	846.5 (0.26)
14		a″	945.8 (0.01)	a″	940.4 (0.00)
15		a′	1029.5 (0.10)	a′	1039.6 (0.10)
16	1087.1 (0.15)	a′	1110.4 (0.28)	a′	1109.4 (0.16)
17	1152.4 (0.38)	a′	1173.6 (0.59)	a′	1182.8 (0.61)
18		a′	1227.3 (0.28)	a′	1228.3 (0.22)
19		a′	1285.2 (0.14)	a′	1266.4 (0.02)
20		a′	1316.1 (0.32)	a′	1278.7 (0.30)
21	1372.4 (0.92)	a′	1396.1 (0.54)	a′	1388.7 (1.00)
22	1394.4 (0.31)	a′	1419.9 (1.00)	a′	1421.3 (0.65)
23	1487.1 (0.23)	a′	1522.4 (0.70)	a′	1536.4 (0.83)
24	1492.4 (1.00)	a′	1529.4 (0.83)	a′	1548.4 (0.42)

[a]UB3LYP/6-311G(d,p), unscaled. [b]Relative intensity based on strongest absorption.

An additional intense and broad absorption at 1892.5 cm^{-1} (argon, 4 K), characteristic of the N=C=C str vibration of a ketenimine, indicates the formation of **4l**. In contrast to the photochemistry of the other systems described here, no traces of nitreno radical **5l** could be detected by IR or EPR spectroscopy. Irradiation with visible light ($\lambda > 420$ nm) yields, as expected, the azirine **3l** with the characteristic C=N str. vibration at 1739.1 cm^{-1} (Figure 11).

Discussion

Nitrene EPR Investigation. The EPR spectrum of nitrene **T-1f** ($|D/hc| = 1.108$ cm^{-1}, $|E/hc| = 0.012$ cm^{-1}) has been discussed in detail previously.[20] The D values of the triplet nitrenes **T-1d**−**T-1l** are close to that of **T-1f** in the characteristic range of aryl nitrenes (Table 1).[21] They strongly depend on the spin density at the nitrene center which is influenced by substituent effects. A strong linear correlation between

(21) Wasserman, E. *Prog. Phys. Org. Chem.* **1971**, *8*, 319–36.

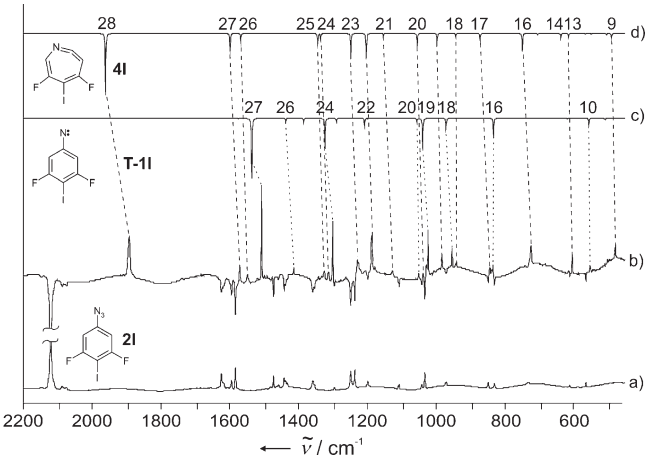

FIGURE 10. IR spectra showing the 254 nm photochemistry of **2l** in argon at 4 K. (a) IR spectrum of **2l** after deposition at 4 K. (b) Difference IR spectrum: bands of **2l** pointing downward disappear; bands pointing upward assigned to **T-1l** and **4l** appear during irradiation. Nitrene radical **5l** was not observed. (c) Calculated IR spectrum of **T-1l**. (d) Calculated IR spectrum of **4l**. All calculations at the (U)B3LYP/6-311G(d,p) level of theory.

SCHEME 6. Photochemistry of 2l

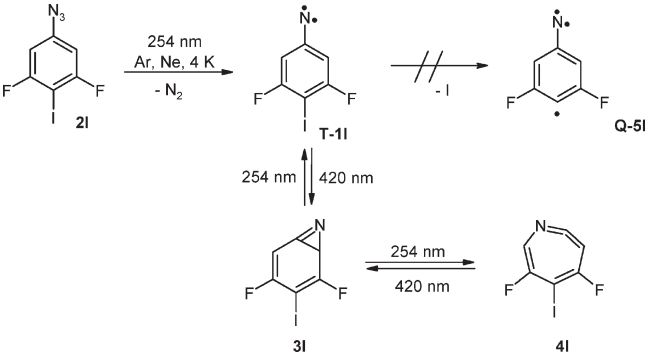

the *D* values of aryl nitrenes and the spin densities at the nitrogen atoms was recently found by Wentrup et al.[9] The *D* values of **T-1d**−**T-1l** only roughly fit into this scheme, since in these nitrenes the influence of the heavy iodine atom on the *D* value has to be taken into account. The zfs parameters of molecules containing heavy atoms are not only influenced by spin−spin dipolar interactions but also by strong spin−orbit coupling (SOC) contributions. The *E* values of **1** are uncommonly large compared to most other arylnitrenes. This also indicates the influence of the iodine substituent on the zfs parameters due to a significant contribution of SOC, in accordance with previous calculations for **T-1f**.[20]

Nitrene Rearrangements. The IR spectra of triplet nitrenes **T-1**, azirines **3**, and ketenimines **4** are in accordance with DFT calculations (Tables 2 and 3 and Table T1, Supporting Information) and agree well with similar molecules described in the literature.[2,13,14,18] The characteristic symmetrical C=C str vibration of the nitrenes **1d**−**k** is found between 1545 and 1597 cm^{-1}. For **T-1l**, the calculated intensity of this vibration is very low, and it could not be observed in the experimental spectrum. For the other nitrenes it was found that the frequency and intensity of this vibration strongly depends on the pattern of the fluorine substitution, in agreement with

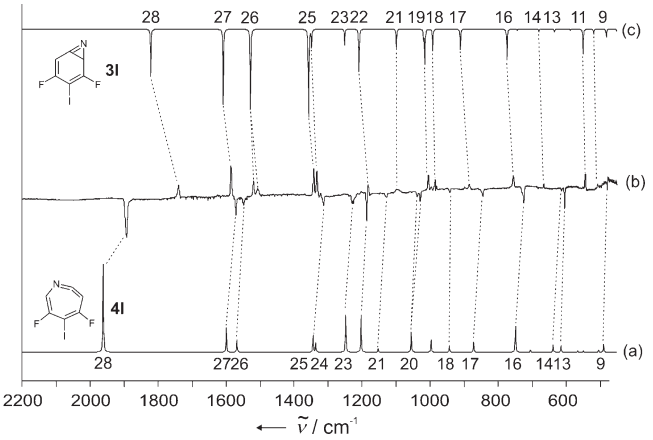

FIGURE 11. IR spectra showing the 420 nm photochemistry of **4l** in argon at 4 K after 30 min irradiation. (a) Calculated IR spectrum of **4l**. b) Difference IR spectrum: bands of **4l** pointing downward disappear; bands pointing upward assigned to **3l** appear during irradiation. (c) Calculated IR spectrum of **3l**. All calculations at the (U)B3LYP/6-311G(d,p) level of theory.

CHART 2. Characteristic C=C=N and C=N Stretching Vibrations of the Ketenimines 6a,[2] 6b−d,[18] and Azirines 7a,b[13] and 7c,d,[18] respectively, Described in the Literature

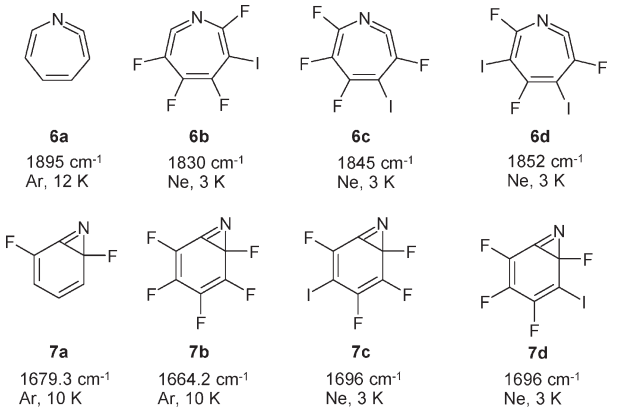

theoretical predictions. The three nitrenes with two *ortho* fluorine substituents show the highest frequency for the symmetrical C=C str vibration. In general, the frequency increases while the intensity decreases with the number of fluorine substituents. The C−N str vibration is also characteristic and found in the spectral range between 1284 and 1363 cm^{-1}. The C3C4C5 deformation vibrations are located in the fingerprint region between 803 and 1056 cm^{-1} (see Supporting Information Table T1).

The C=C=N str vibrations of ketenimines **4** and **4′** are located between 1840.7 and 1893.5 cm^{-1}, in good agreement with similar systems published in the literature (Chart 2). The C=N str vibrations of the azirines **3** and **3′** are found between 1680.8 and 1739.1 cm^{-1} (Table 3).

Phenyl nitrenes with fluorine substituents initially were regarded as photochemically stable.[22] Later it was shown that selective photolysis of fluorinated phenylnitrenes produces azirines[13] and ketenimines, although fluorination markedly increases the photostability of the nitrenes.[18,14]

(22) Dunkin, I. R.; Thomson, P. C. P. *J. Chem. Soc., Chem. Commun.* **1982**, 1192–1193.

Hayes and Sheridan[2] observed that phenylnitrene and ketenimine are formed with a constant initial ratio, regardless which matrix was used, which indicates that these products interconvert and are formed in photostationary equilibria. The increased stability of fluorinated phenylnitrenes results in higher yields of the nitrenes in the product mixtures. The thermal barrier for the addition of the nitrogen atom into adjacent C−C bonds is predicted to be 3.5−4.5 kcal/mol higher for the *ortho*-fluorinated systems than for the parent phenylnitrene.[12] Platz et al. found that the rearrangement of phenylnitrene takes place on the excited π^2 state of the singlet nitrene. This state is destabilized by fluorine substituents, and hence these rearrangements become less favored.[23] This interpretation was later supported by DFT calculations of Smith and Cramer.[24] The photochemistry of phenylnitrene with one fluorine atom in *ortho* position was studied by Gritsan et al. with laser flash photolysis and theoretical methods. Evidence was presented that the azirine is an intermediate and that the corresponding singlet nitrene and azirine interconvert in solution.[25]

Our results are in accordance with these studies. In all cases, selective irradiations result in the interconversion between nitrene **1**, azirine **3**, and ketenimine **4**. However, unsymmetrical substitution leads to the preferential formation of isomers that cannot be easily understood. A complication for the interpretation of the experimental results is that there is no simple way to discriminate between true photochemical reactions and hot ground state reactions. In the latter case, the thermal deactivation of electronically excited states results in thermally excited molecules which undergo subsequent thermal rearrangements. To understand the thermal pathways we calculated the relative energies of the isomers and the activation barriers at the ((U)B3LYP/6-311G(d,p)) level of theory. Interestingly, there is a correlation between the activation barriers for the ring closure of the nitrenes **1** and the relative yields of the isomeric azirines **3**, **3′** in the matrix. In contrast, the yields of the ketenimines **4**, **4′** correlate with their relative stabilities (Table 10, Figure 12, Supporting Information Figures S5−S8).

The nitrenes **1** are produced by UV irradiation (254 nm) of the azides **2** in yields depending on the constitution of the nitrene and the irradiation conditions. Since phenylnitrenes are stabilized by *ortho* fluorine substituents, the yield of **1** is highest with two *ortho* fluorine atoms and smallest without fluorine atoms in *ortho* positions. Visible light irradiation of the nitrenes **1** produces azirines, whereas prolonged UV irradiation yields the ketenimines.

The influence of one *ortho* fluorine substituent on the relative yields of the isomeric azirines **3** and **3′** and the isomeric ketenimines **4** and **4′** is most pronounced for **1h** and **1k**. Visible light irradiation (420 nm) produces exclusively azirine **3′h** by formal insertion of the nitrogen atom away from the *ortho* fluorine substituent. The calculated barrier for the formation of **3′h** is 22.8 kcal/mol, while that for **3h** is 27.5 kcal/mol. At the same level of theory **3h** is calculated to be more stable than **3′h** by 4.3 kcal/mol. This is in accordance with earlier theoretical studies on fluorinated phenylnitrenes.[25] A careful inspection of the experimental results reveals a general trend: the isomer of the azirine that is preferentially formed is the kinetically favored but thermodynamically less stable isomer; thus, the photochemical rearrangements follow the thermal activation barriers.

TABLE 10. Energies (kcal mol^{-1}) of the Rearrangement Products and Their Transition States Relative to S-1 (B3LYP/6-311G(d,p))

	TS1	TS1′	3	3′	TS2	TS2′	4	4′
2,6- (**d**)	26.0		10.4		16.5		3.2	
2,3,6- (**e**)	24.6	26.7	6.8	10.0	16.0	15.3	4.5	−1.9
2,3,5,6- (**f**)	24.7		5.1		12.7		−1.5	
2,3,5- (**g**)	26.0	23.3	4.1	12.8	10.1	20.9	−1.8	5.7
2,5- (**h**)	27.5	22.8	8.8	13.1	12.5	23.1	−3.0	11.5
2,3- (**i**)	25.7	23.3	4.8	15.1	11.3	21.1	1.4	3.8
2- (**k**)	27.3	22.6	8.9	14.7	12.4	22.1	−0.3	9.5
3,5- (**l**)		23.6		10.3		16.1		4.0

UV irradiation (254 nm) of nitrene **1h** produces ketenimine **4h** but not **4′h**. This is striking since the preferred azirine **3′h** is expected to rearrange to **4′h** via ring-opening. DFT calculations reveal that ketenimine **4h** with no fluorine atom attached to the cumulene double bond is considerably more stable than isomer **4′h** and that the barrier for its formation via ring-opening from azirine **3h** is also lower (Figure 12a, Table 10). The same is true for **4k** and **4′k**. On the other hand, the difference between both barriers for the ring-opening from azirine **3i** and **3′i** to **4i** and **4′i**, respectively, and particularly between the energies of **4i** and **4′i** are much less pronounced (Supporting Information, Figure S6 and Table 10). The experimental results show that **4i** and **4′i** are formed in comparable yields in the matrix upon 254 nm irradiation. The barriers of the ring-opening to form **4k** and **4′k**, respectively, differ in a similar way than those for the formation of **4e** and **4′e**, but the difference in their thermodynamic stability is more pronounced for **4k** and **4′k**. Since **4′k** could not be isolated in the matrix at all, the selectivity of the ring-opening reaction seems to be thermodynamically controlled and the thermal barriers for the ring-opening of **3** are less related to the distribution of the isomers of **4**.

Irradiation of **4g** with visible light (420 nm) produces **3g** as a major product, the isomer that is obtained only as a minor product of the visible light irradiation of nitrene **1g**. Thus, by selecting the sequence of irradiations, either **3g** or **3′g** can be obtained as the major product. This suggests that there is no photostationary equilibrium between the isomers of **1g**, in particular not between **3g** and **3′g**.

There are two possible mechanisms for the formation of **4g** via UV irradiation of **1g**: (i) **3g** is formed as an intermediate with a low stationary concentration that subsequently rearranges to **4g** or (ii) **4g** is directly formed from **1g** without passing **3g** as intermediate. Although there is no direct evidence, mechanism (ii) seems to be more plausible since (i) requires a switch in the selectivities by changing the irradiation wavelength which is difficult to understand.

In some cases, the less stable ketenimine can be obtained by irradiating the corresponding azirine with UV light. This is especially striking for **1g** where the more stable ketenimine **4g** is almost the only product formed after UV irradiation. However, **4′g** can be synthesized as minor products by irradiating **3′g** with UV light, although most of the **3′g** reacts back to the nitrene under these conditions.

(23) Platz, M. S. *Acc. Chem. Res.* **1995**, *28*, 487–492.
(24) Smith, B. A.; Cramer, C. J. *J. Am. Chem. Soc.* **1996**, *118*, 5490–5491.
(25) Gritsan, N. P.; Gudmundsdottir, A. D.; Tigelaar, D.; Zhu, Z.; Karney, W. L.; Hadad, C. M.; Platz, M. S. *J. Am. Chem. Soc.* **2001**, *123*, 1951–1962.

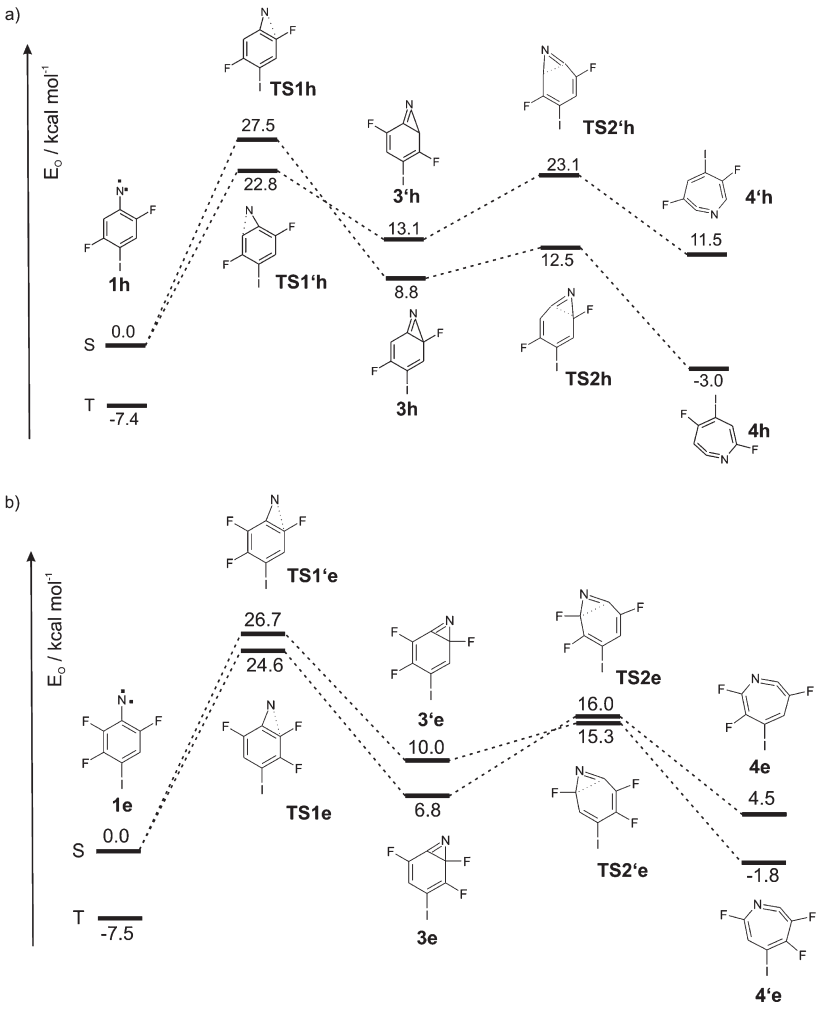

FIGURE 12. Relative energies of the rearrangement products and transition states of (a) **1h** and)b) **1e**.

An interesting case of selectivity is nitrene **1e** with two fluorine atoms in the *ortho* position but only one in the *meta* position. The calculations predict that azirine **3e** is 3.2 kcal/mol more stable and the barrier for its formation is 2.1 kcal/mol lower than that of its isomer **3′e** (Figure 12b). Of the two ketenimines, **4′e** is more stable by 6.4 kcal/mol. Again, a selective photochemistry is observed: UV irradiation of **1e** preferentially produces the most stable ketenimin isomer **4′e**, whereas visible light irradiation gives mainly azirine **3e**, which is formed by ring closure of the nitrene with a lower barrier than **3′e** (in this case it is also thermodynamically more stable than its isomer **3′e**).

Of all systems investigated in this study, **1k** shows the highest selectivity. While in most systems the less stable ketenimine and the azirine with the higher barrier for ring closure from the nitrene are also formed as minor products, **3′k** and **4k** are formed exclusively without any trace of **3k** and **4′k** detectable in the matrix.

Although details of the mechanism of the formation of azirines **3** and ketenimines **4** are not known, it is obvious that DFT calculations of the relative stabilities of the isomers and of the barriers for their formation can be used to predict the distribution of isomers even in a semiquantitative way. A larger difference in the thermal stability or the activation barriers, respectively, results in a larger preference of one of the isomers.

Nitreno Radicals Q-5. Nitreno radicals **5** are an interesting class of high-spin molecules with a quartet ground state. The electronic structure of a nitreno radical **5** is described best as a σ,σ,π-triradical with one unpaired electron located at a σ orbital at the nitrogen atom, one at a σ orbital at the *para* carbon atom, and one delocalized in the π system.[17] This delocalized unpaired π electron accounts for a partial nitrene character at the nitrogen atom and partial carbene character at the *para* carbon atom. To retain the local high-spin characters of the nitrene and carbene centers, a quartet state is energetically favored for the overall spin system.[20]

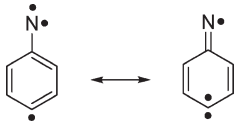

EPR signals of the nitreno radicals **5** are observed during 308 nm irradiation (XeCl excimer laser) of the precursors at 4−15 K. Annealing at 30 K results in the disappearance of these signals and subsequent 308 nm irradiation at 4 K in their reappearance. This behavior is characteristic of radical pairs produced by photolysis of matrix isolated precursors. The radical pair is formed in a matrix cage, and annealing leads to rapid thermal radical recombination. Nitrenes **1** and

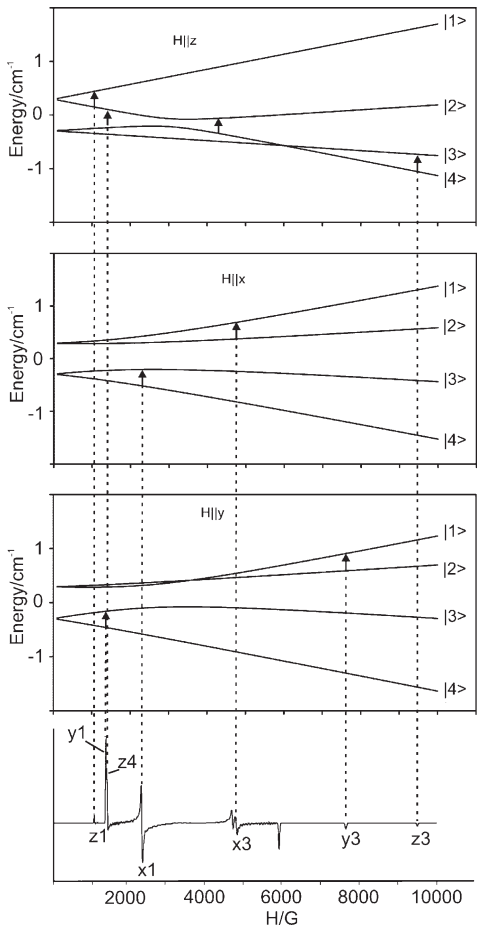

FIGURE 13. Energy of the four quartet sublevels of the external field H parallel to z, x, and y-axes, respectively, calculated for a quartet system using the zfs parameters $|D/hc| = 0.285$ cm^{-1}, $|E/hc| = 0.043$ cm^{-1} ($g_{iso} = 2.003$) of **Q-5f** as a representative example for the assignment of the transitions of the nitrino radicals in this study.

the other intermediates do not show this behavior (no reaction with N_2 under the conditions of matrix isolation) which allows to assign signals of the nitreno radicals **5** even if the yield is low.

The EPR spectra of **Q-5** could be reproduced by simulation of quartet high-spin systems with suitable zfs parameters, which allows the assignment of all experimentally observed EPR transitions. For **Q-5f** the zfs parameters $|D/hc| = 0.285$ and $|E/hc| = 0.043$ cm^{-1} were reported previously.[20] The field dependence of the magnetic energy levels of **5f** was calculated for the principal axes using the solution of the Hamilton matrix of a quartet state[26,27] with the parameters derived from the simulation (Figure 13). Two signals cannot be assigned to axial transitions. These off-axis transitions are typical for EPR spectra of high-spin systems with $S > 1$. The zfs parameters of the quartet nitreno radicals **Q-5d**−**Q-5k** are quite similar. The D and E values are found in narrow ranges between 0.278 and 0.29 cm^{-1} and 0.040 and 0.043 cm^{-1}, respectively (Table 1). The small differences in the appearance of the EPR spectra are explained by the field dependence of the transitions as

(26) Rai, U. S.; Symons, M. C. R.; Wyatt, J. L.; Bowman, W. R. *J. Chem. Soc., Faraday Trans.* **1993**, *89*, 1199–201.

(27) Atherton, N. M. *Principles of Electron Spin Resonance*; Prentice Hall: New York, 1993.

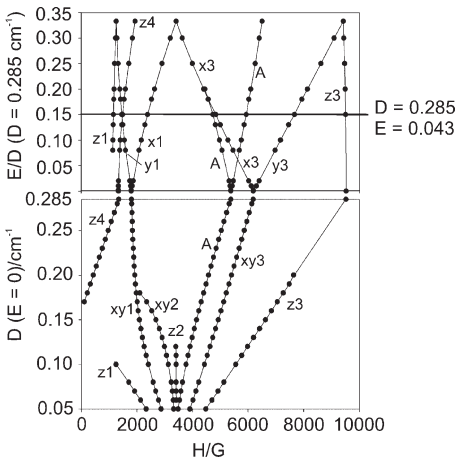

FIGURE 14. Simulation of the field dependence of the most intense axial transitions of a quartet system with D values between 0.05 and 0.285 cm^{-1} and E/D between 0 and 0.35. The values $|D/hc| = 0.285$ and $|E/hc| = 0.043$ cm^{-1} of **5f** are marked.

a function of the zfs parameters (Figure 14). The most noticeable difference between the quartet spectra are observed in the low-field region for the transitions z4 and y1. While for **Q-5 h** transition z4 appears at lower field than y1 (Figure 8), for **Q-5d** with a slightly larger D value it is located at higher field than y1 (Figure 4). The zfs parameters in nitreno radicals are largely dominated by one-center spin−spin interactions,[20] and since the spin densities at the nitrene and the carbene centers in **Q-5** show only small variations, similar zfs parameters can be expected for all nitreno radicals (Table 11).

Calculations show that the magnetic z-axis of the quartet nitreno radical is located parallel to the N−C bond, the x-axis is perpendicular to the molecular plane, and the y-axis lies in the molecular plane. Thus, the nitrene character prevails over the carbene character. However, the carbene character is reflected by an enhanced dipolar field in the y-direction which is sufficiently strong to give significant magnetically inequivalent y- and x-directions. Thus, the nonzero E-value in **Q-5f** and the other nitreno radicals mainly reflects the carbene character of the system. This carbene character, in turn, is controlled by the properties of the π-system since the out-of-plane spin-density arises from the conjugation of the nitrene out-of-plane SOMO and the π-system of the ring.[20]

To synthesize the nitreno radicals in argon matrices the corresponding azides **2** have to be irradiated with UV light (254 nm). Under these conditions, the formation of **5** competes with the rearrangement to the ketenimines **4**. Only nitrenes **1** with one or two fluorine atoms in the *ortho* positions are stable enough toward rearrangement to produce nitreno radicals **5** in yields high enough to allow their spectroscopic detection. Thus, nitreno radical **5l** could be detected neither by IR nor by the more sensitive EPR spectroscopy.

The formation of nitreno radicals **5** is most efficient in argon at 4 K, whereas at 10 K or in neon at 4 K the yields are much lower. In several instances, the nitreno radicals could be detected in argon at 10 K only by EPR, but not by IR spectroscopy, whereas at 4 K clear IR signals were obtained. This is probably related to the immobilization of radical pairs (**5** and the iodine atom) in the matrix cages. A slight

TABLE 11. Spin Densities at the Nitrene and the Carbene Centers of Q-5

	spin density[a]	
Q5	at N	at C4
2,3,5,6- (**f**)	1.5771	1.2480
2,3,6- (**e**)	1.5749	1.2420
2,6- (**d**)	1.5739	1.2398
2,3,5- (**g**)	1.5803	1.2565
2,5- (**h**)	1.5709	1.2586
2,3- (**i**)	1.5811	1.2452
2- (**k**)	1.5742	1.2493

[a]UB3LYP/6-311G(d,p).

increase of the temperature results in an efficient recombination of the radical pair under formation of **1**. The effect of argon vs neon matrices is not understood, we can only speculate that the different shape of matrix cages in these rare gases influences the stability of the radical pairs.

Theoretical studies with 4-dehydrophenylnitrene have shown that the ground state of **5a** is the $^4A_2$ state, only 2−5 kcal/mol lower in energy than the lowest lying doublet state, which is a $^2A_2$ state.[17] Thus, the lowest-energy doublet state of **5a** has the same electronic configuration as the quartet ground state. The geometries of both states are quite similar and show only minor bond length alternation, mostly reflected in a 0.028 Å longer C−N bond in the doublet geometry. Similar results are found for the geometries and infrared spectra of the nitreno radicals **5d**−**l**. In Figure 15 the geometries of the $^4A_2$ state of **Q-5d** and the $^2A_2$ state of **D-5d** are shown as typical examples for nitreno radicals. Both C_{2v} symmetrical states show almost similar bond lengths and bond angles. As a consequence, the calculated doublet and quartet infrared spectra are very similar with only small frequency shifts (Table 4). This makes it difficult to determine the spin state of these nitreno radicals by infrared spectroscopy, in particular since only the strongest bands are visible in the experiment. Hence, only EPR spectroscopy, which is very sensitive to paramagnetic species, proves the quartet state of the nitreno radicals. An interesting case is **5f**, where the doublet state has a nonplanar C_S symmetrical geometry, while **Q-5f** is planar with C_{2v} symmetry. As a result, the calculated IR spectra of the quartet and doublet states of **5f** are different enough and allowed a definitive assignment of the electronic state of **5f** based only on IR spectroscopy.[19]

Experimental Section

Synthesis. All phenyl azides were synthesized in analogy to the synthesis of 2,3,4,5-tetrafluoroaniline and 2,3,4,5-tetrafluorophenylazide described in the literature.[19] The 2,6-difluoro-4-iodoaniline was synthesized starting from 2,6-difluoroaniline according to a procedure described by Kutepov et al.[28] The synthetic, spectroscopic, and analytical data are given in the Supporting Information.

Matrix Isolation. Matrix isolation experiments were performed by standard techniques[29] with closed cycle helium cryostats allowing cooling of a CsI spectroscopic window to 4 K. FTIR spectra were recorded with a standard resolution of 0.5 cm^{-1}, using a N_2(*l*)-cooled MCT detector in the range 400−4000 cm^{-1}. X-band EPR spectra were recorded with a Bruker Elexsys E500 EPR spectrometer with an ER077R magnet (75 mm pole cap distance), an ER047 XG-T microwave bridge, and an oxygen-free high-conductivity copper rod (75 mm length, 3 mm diameter) cooled by a closed-cycle cryostat.

Broadband irradiation was carried out with mercury high-pressure arc lamps in housings equipped with quartz optics and dichroic mirrors in combination with cutoff filters (50% transmission at the wavelength specified). IR irradiation from the lamps was absorbed by a 10 cm path of water. For 254 nm irradiation a low pressure mercury arc lamp was used. A XeCl excimer laser was used for 308 nm irradiation.

Computational Methods. Optimized geometries and vibrational frequencies of all species were calculated with the Gaussian 03 suite of programs.[30] The computer simulation of the EPR spectrum was performed by using the XSophe computer simulation software suite (version 1.0.4),[31] developed by the Centre for Magnetic Resonance and Department of Mathematics, University of Queensland, Brisbane, Australia, and Bruker Analytik GmbH, Rheinstetten. Germany.

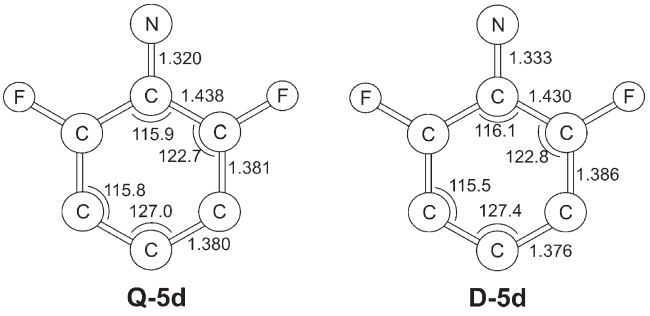

FIGURE 15. Geometries of the $^4A_2$ state of **Q-5d** and the $^2A_2$ state of **D-5d** on the UB3LYP/6-311G(d,p) level of theory. Both states show C_{2v} symmetry and the bond lengths and angles, as well as the calculated IR spectra, are quite similar.

Acknowledgment. This work was financially supported by the Deutsche Forschungsgemeinschaft and the Fonds der Chemischen Industrie.

Supporting Information Available: Additional figures and tables; synthetic, spectroscopic, and analytical data. Geometries, total energies, and IR spectroscopic data of the photoproducts. Relative energies of all rearrangement products; ^1H and ^{13}C NMR spectra. This material is available free of charge via the Internet at http://pubs.acs.org.

(28) Kutepov, D. F.; Khokhlov, D. N.; Tuzhilkina, V. L. *Zh. Obsh. Khim.* **1960**, *30*, 2484–9.

(29) Dunkin, I. R. *Matrix Isolation Techniques: A Practical Approach*; Oxford University Press: Oxford, 1998.

(30) Frisch, M. J. T.; Trucks, G. W.; Schlegel, H. B.; Scuseria, G. E.; Robb, M. A.; Cheeseman, J. R.; Montgomery, Jr., J. A.; Vreven, T.; Kudin, K. N.; Burant, J. C.; Millam, J. M.; Iyengar, S. S.; Tomasi, J.; Barone, V.; Mennucci, B.; Cossi, M.; Scalmani, G.; Rega, N.; Petersson, G. A.; Nakatsuji, H.; Hada, M.; Ehara, M.; Toyota, K.; Fukuda, R.; Hasegawa, J.; Ishida, M.; Nakajima, T.; Honda, Y.; Kitao, O.; Nakai, H.; Klene, M.; Li, X.; Knox, J. E.; Hratchian, H. P.; Cross, J. B.; Bakken, V.; Adamo, C.; Jaramillo, J.; Gomperts, R.; Stratmann, R. E.; Yazyev, O.; Austin, A. J.; Cammi, R.; Pomelli, C.; Ochterski, J. W.; Ayala, P. Y.; Morokuma, K.; Voth, G. A.; Salvador, P.; Dannenberg, J. J.; Zakrzewski, V. G.; Dapprich, S.; Daniels, A. D.; Strain, M. C.; Farkas, O.; Malick, D. K.; Rabuck, A. D.; Raghavachari, K.; Foresman, J. B.; Ortiz, J. V.; Cui, Q.; Baboul, A. G.; Clifford, S.; Cioslowski, J.; Stefanov, B. B.; Liu, G.; Liashenko, A.; Piskorz, P.; Komaromi, I.; Martin, R. L.; Fox, D. J.; Keith, T.; Al-Laham, M. A.; Peng, C. Y.; Nanayakkara, A.; Challacombe, M.; Gill, P. M. W.; Johnson, B.; Chen, W.; Wong, M. W.; Gonzalez, C.; Pople, J. A. *Gaussian 03, Revision C.02*; Gaussian, Inc.: Wallingford CT, 2004.

(31) Griffin, M.; Muys, A.; Noble, C.; Wang, D.; Eldershaw, C.; Gates, K. E.; Burrage, K.; Hanson, G. R. *Mol. Phys. Rep.* **1999**, *26*, 60–84.